

Supporting Information

Quantitative Temporally and Spatially Resolved X-ray Fluorescence Microprobe Characterization of the Manganese Dissolution-Deposition Mechanism in Aqueous Zn/ α -MnO₂ Batteries

Daren Wu^{1†}, Lisa M. Housel[†], Sung Joo Kim^{3,4}, Nahian Sadique², Calvin D. Quilty², Lijun Wu⁴, Ryan Tappero⁵, Sarah L. Nicholas⁵, Steven Ehrlich⁵, Yimei Zhu^{4,6}, Amy C. Marschilok^{1,2,3}, Esther S. Takeuchi^{1,2,3*}, David C. Bock^{3*}, Kenneth J. Takeuchi^{1,2*}

¹Department of Materials Science and Chemical Engineering, Stony Brook University, Stony Brook, New York 11794, United States

²Department of Chemistry, Stony Brook University, Stony Brook, New York 11794, United States

³Energy and Photon Sciences Directorate, Brookhaven National Laboratory, Upton, New York 11973, United States

⁴Condensed Matter Physics and Materials Science Department, Brookhaven National Laboratory, Upton, New York 11973, United States

⁵National Synchrotron Light Source II, Brookhaven National Laboratory, Upton, New York 11973, United States

⁶Department of Physics and Astronomy, Stony Brook University, Stony Brook, New York 11794, United States

* corresponding authors: (EST) esther.takeuchi@stonybrook.edu, (DCB) dbock@bnl.gov, (KJT) kenneth.takeuchi.1@stonybrook.edu

†authors contributed equally to the manuscript

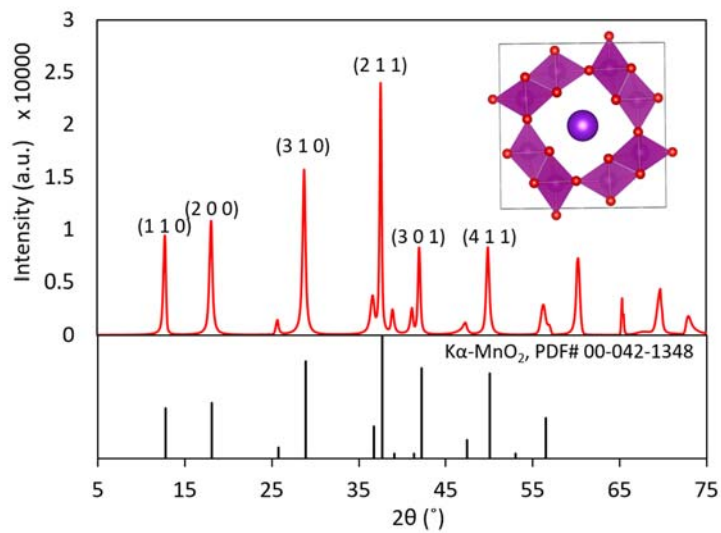


Figure S1. XRD pattern of synthesized α -MnO₂.

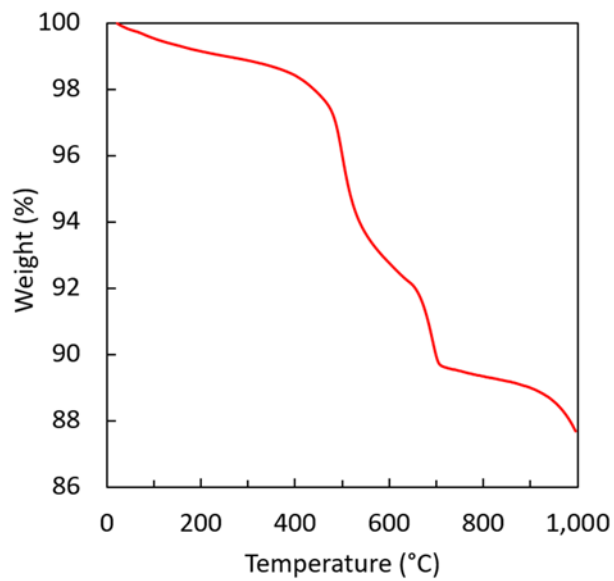


Figure S2. TGA of synthesized α -MnO₂.

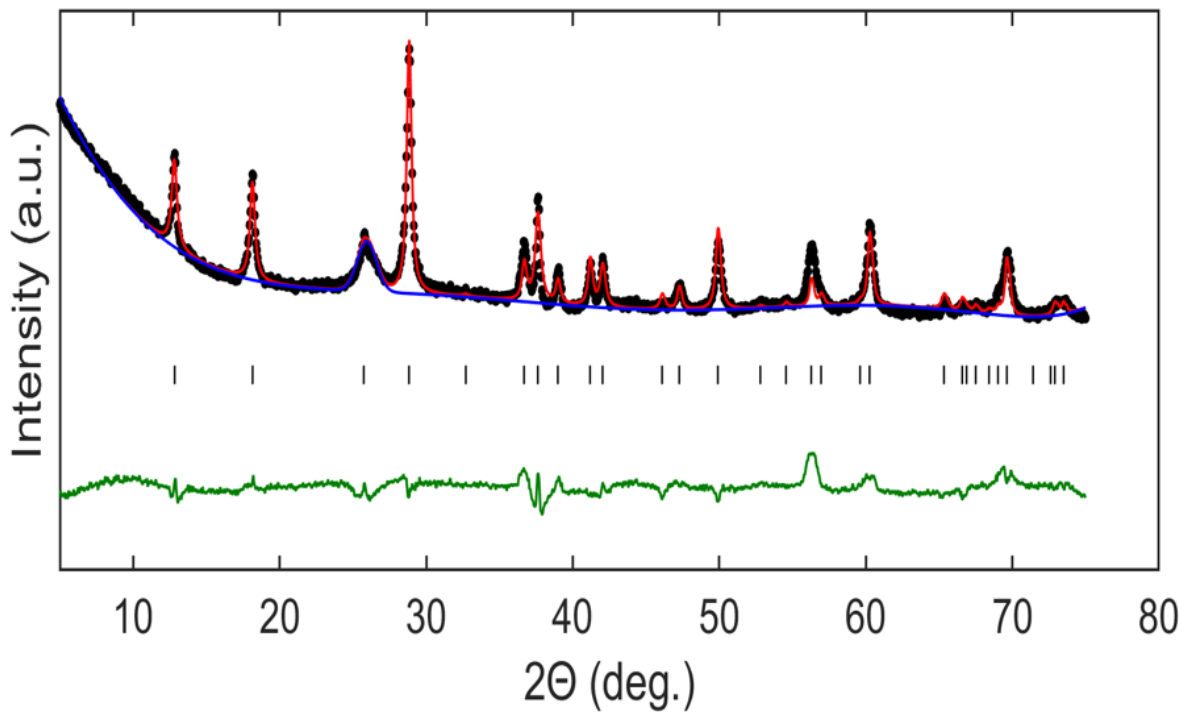


Figure S3. Rietveld refinement of XRD for pristine α -MnO₂/CNT electrode where black points represent experimental data, red line is the calculated fit, blue line is background, and green line is the difference between the observed and calculated data. Black reference lines are based on PDF # 00-020-0908. The intense peak at $\sim 25^\circ$ due to the presence of the CNT was incorporated as part of the background.

Parameter	Value
Space group	I 4/m
$a(\text{\AA})$	9.81(3)
$c(\text{\AA})$	2.85(3)
Crystallite size (nm)	Equatorial=21(.7) Axial=16(.9)
K ⁺ (occupancy)	0.345
%Rwp	3.205

Table S1. Rietveld refinement results for pristine α -MnO₂/CNT electrode.

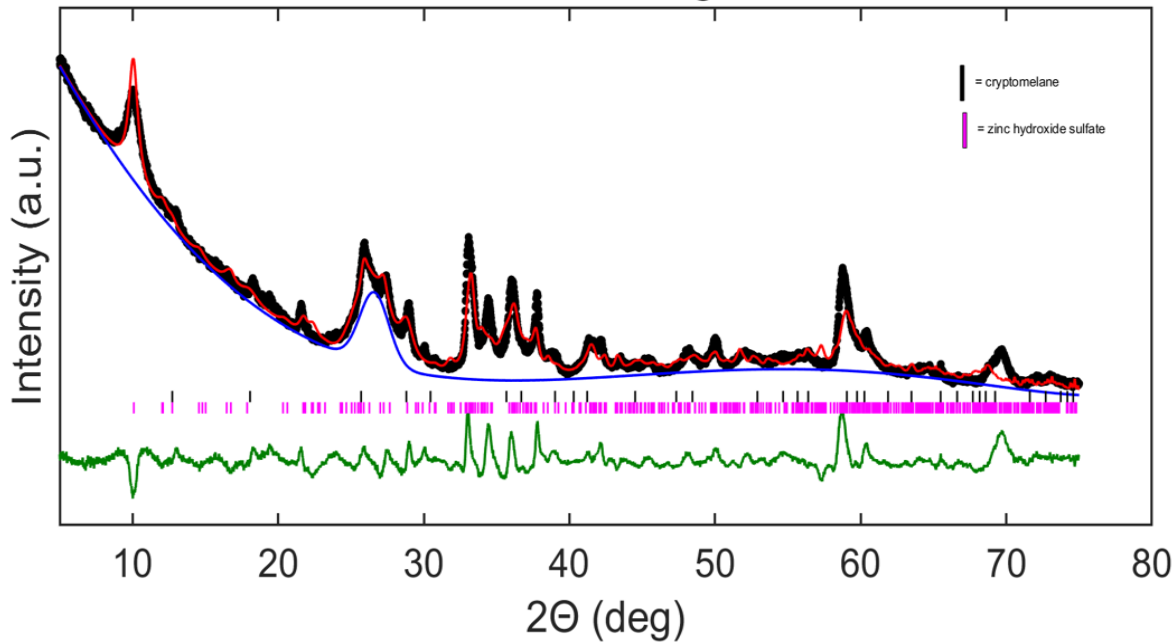


Figure S4. Rietveld refinement of XRD of 1st cycle discharged cathode with α -MnO₂ (cryptomelane) and ZHS phase where black points represent experimental data, red line is the calculated fit, blue line is background, and green line is the difference between the observed and calculated data. Reference lines are PDF #00-020-0908 for cryptomelane (black) and PDF #00-067-0055 for ZHS (pink). The intense peak at $\sim 25^\circ$ due to the presence of the CNT was incorporated as part of the background.

Parameter	Value (cryptomelane)	Value (ZHS)
Space group	I 4/m	P-1
$a(\text{\AA})$	9.76(7)	8.2(11)
$b(\text{\AA})$		8.2(12)
$c(\text{\AA})$	3.06(3)	8.88(8)
$\alpha=$		99.49(5)
$\beta=$		79.3(2)
$\gamma=$		117.4(2)
Crystallite size (nm)	Equatorial=6(.5) Axial=5(4)	11(.3)
Weight Fraction	64%(4)	36%(8)
K ⁺ (occupancy)	0.2(3)1	
%Rwp		6.230

Table S2. Rietveld refinement results for the 1st discharged cathode.

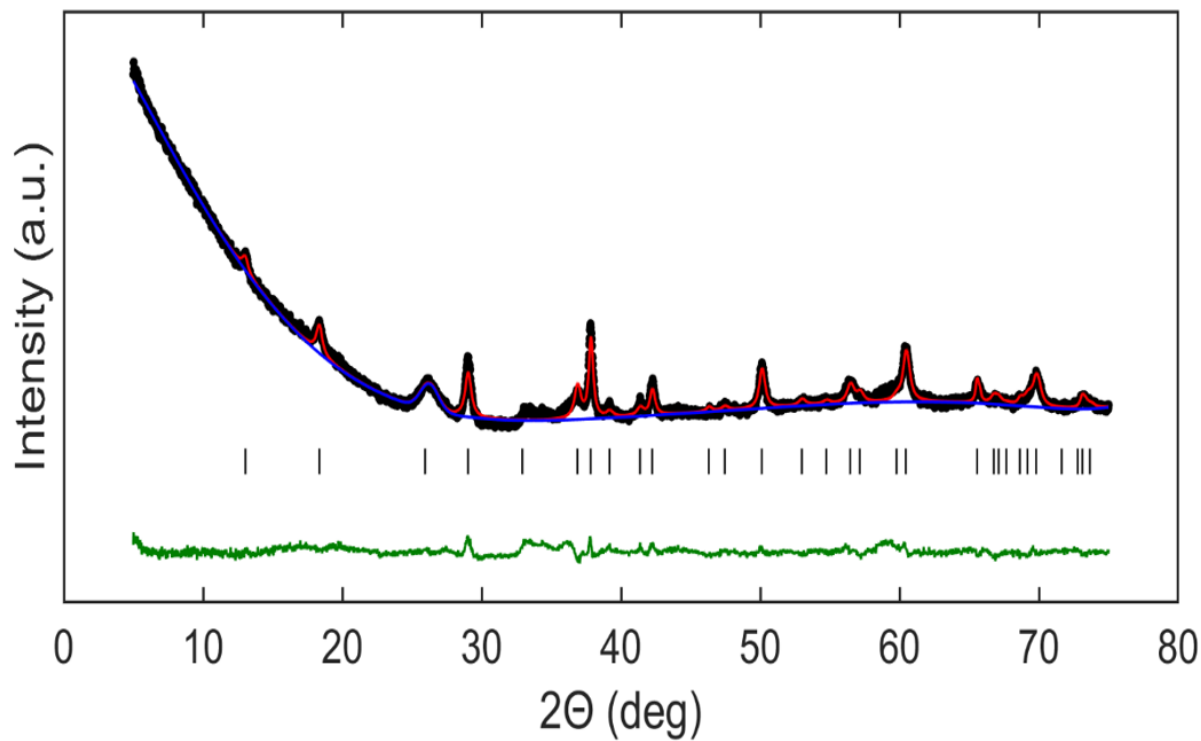


Figure S5. Rietveld refinement of XRD of 1st cycle charged cathode where black points represent experimental data, red line is the calculated fit, blue line is background, and green line is the difference between the observed and calculated data. Black reference lines are based on PDF #00-020-0908 for cryptomelane. The intense peak at ~25° due to the presence of the CNT was incorporated as part of the background.

Parameter	Value
Space group	I 4/m
$a(\text{\AA})$	9.82(2)
$c(\text{\AA})$	2.856(3)
Crystallite size (nm)	Equatorial=19(4) Axial=55(5)
K ⁺ (occupancy)	0.2(1)2
%Rwp	2.539

Table S3. Rietveld refinement results for 1st cycle charged cathode.

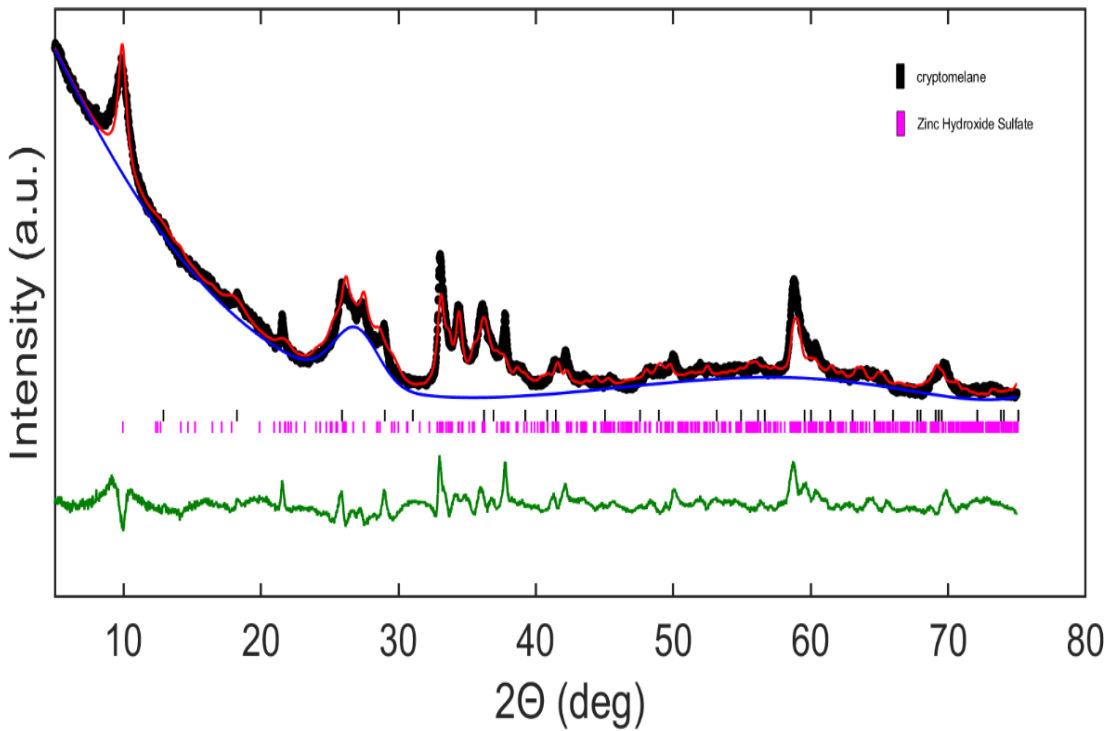


Figure S6. Rietveld refinement of XRD of 5th cycle discharged cathode with α -MnO₂ phase (cryptomelane) and ZHS phase. The black points represent the experimental data, the red line is the calculated fit, the blue line is the background, and the green line is the difference between the observed and calculated data. The reflections lines are based on PDF #00-020-0908 for cryptomelane and PDF # 00-067-0055 for ZHS. The intense peak at $\sim 25^\circ$ due to the presence of the CNT was incorporated as part of the background.

Parameter	Value (cryptomelane)	Value (ZHS1)
Space group	I 4/m	P-1
$a(\text{\AA})$	9.7(4)	8.3(2)
$b(\text{\AA})$		8.3(2)
$c(\text{\AA})$	3.01(3)	9.2(2)
$\alpha=$		100.4(5)
$\beta=$		77.0(4)
$\gamma=$		119.8(3)
Crystallite size (nm)	Equatorial=4(5) Axial=9(3)	11(4)
Weight Fraction	41.6%(3.2)	58.4%(1.2)
K ⁺ (occupancy)	0.055	
%Rwp		5.224

Table S4. Rietveld refinement results for the 5th cycle discharged cathode.

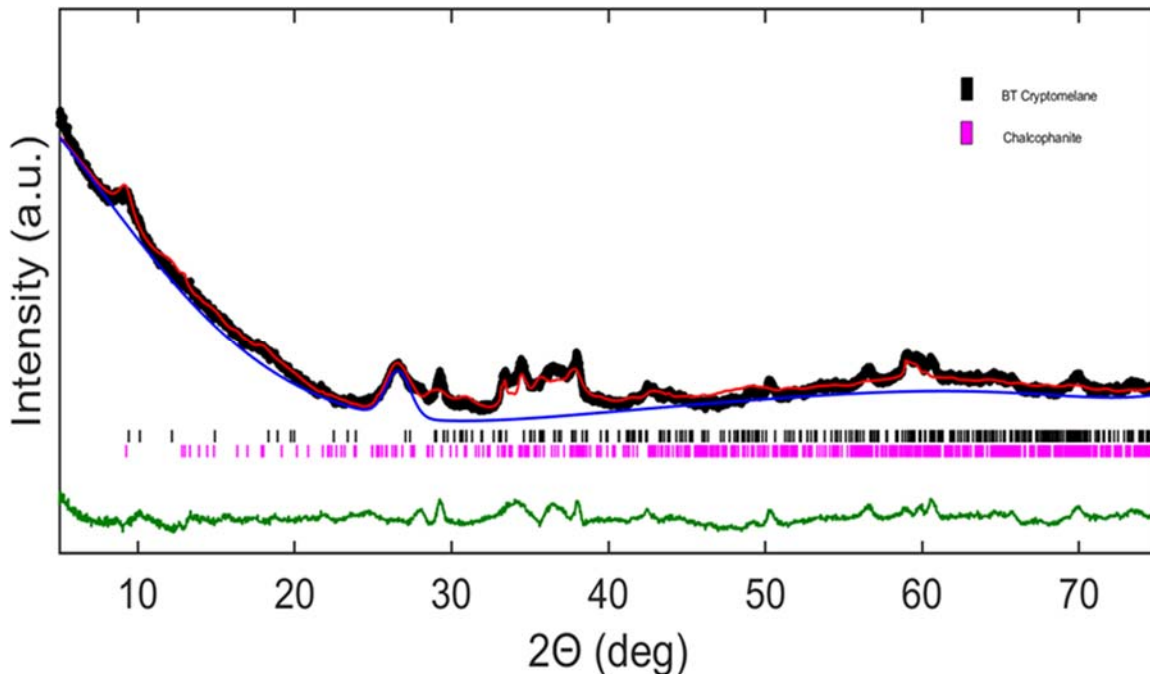


Figure S7. Rietveld refinement of XRD pattern collected of 5th cycle charged cryptomelane with the Broken tunnel cryptomelane phase and chalcophanite phase. The black points represent the experimental data, the red line is the calculated fit, the blue line is the background, and the green line is the difference between the observed and calculated data. The reflections lines are based on the broken tunnel cryptomelane phase in black and the chalcophanite phase in pink. The intense peak at $\sim 25^\circ$ due to the presence of the CNT was incorporated as part of the background.

Parameter	Value (BT - cryptomelane)	Value (Chalcophanite)
Space group	<i>P-1</i>	<i>P-1</i>
<i>a</i> (Å)	10.2(9)5	8.3(8)1
<i>b</i> (Å)	9.4(7)0	8.3(7)3
<i>c</i> (Å)	3.15(3)	11.(1)81
α =	89.0(5)	96.(1)27
β =	94.(1)00	112.(1)48
γ =	102.(3)85	119.9(7)4
Crystallite size (nm)	Equatorial=5(.2) Axial=18(3)	Equatorial=>90 Axial=8(.5)
Weight Fraction	75.7% (1)	24.3%(1)
%Rwp		4.066

Table S5. Rietveld refinement results for the 5th cycle charged cathode.

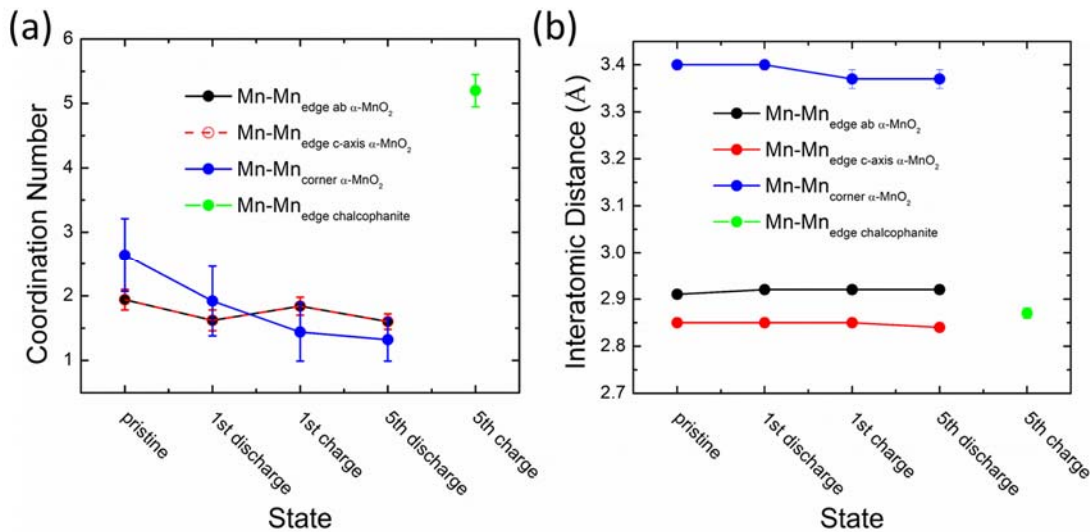


Figure S8. (a) Coordination number and (b) interatomic distances for Mn-Mn paths determined from EXAFS fits of pristine and (dis)charged MnO_2 electrodes.

Sample	Oxidation state from LCF	Expected specific capacity based on measured oxidation state from LCF (mAh/g)	Actual specific capacity measured from electrochemistry (mAh/g)
Pristine	3.880	N/A	N/A
1 st discharge	3.603	81	300
1 st charge	3.741	40	227
5 th discharge	3.468	N/A	211
5 th charge	3.672	60	200

Table S6. Specific capacity comparison between the calculated values from LCF determined oxidation state and actual values from electrochemistry. The specific capacity based on oxidation state was calculated assuming a theoretical molecular weight of 734.6 g/mol and assuming no dissolution of Mn.

Path	E_0	Coordination Number	Interatomic Distance (Å)	σ^2 (x 10 ⁻³ Å ²)
Mn-O	1.0 ± 0.8	2.91 ± 0.24	1.88 ± 0.01	2.4 ± 0.9
	1.0 ± 0.8	2.91 ± 0.24	1.92 ± 0.01	2.4 ± 0.9
	1.0 ± 0.8	1.94 ± 0.16	2.85 ± 0.01	2.4 ± 0.9
	1.0 ± 0.8	1.94 ± 0.16	2.91 ± 0.01	2.4 ± 0.9
	1.0 ± 0.8	2.91 ± 0.24	3.44 ± 0.01	2.4 ± 0.9
	1.0 ± 0.8	3.88 ± 0.32	3.47 ± 0.01	2.4 ± 0.9
	1.0 ± 0.8	2.64 ± 0.57	3.40 ± 0.01	2.4 ± 0.9
Mn-Mn _{edge c-axis}	0.4 ± 0.9	2.43 ± 0.24	1.88 ± 0.01	1.9 ± 1.1
	0.4 ± 0.9	2.43 ± 0.24	1.92 ± 0.01	1.9 ± 1.1
	0.4 ± 0.9	1.62 ± 0.16	2.85 ± 0.01	1.9 ± 1.1
	0.4 ± 0.9	1.62 ± 0.16	2.91 ± 0.01	1.9 ± 1.1
	0.4 ± 0.9	2.43 ± 0.24	3.43 ± 0.01	1.9 ± 1.1
	0.4 ± 0.9	3.24 ± 0.32	3.45 ± 0.01	1.9 ± 1.1
	0.4 ± 0.9	1.92 ± 0.54	3.40 ± 0.02	1.9 ± 1.1
Mn-Mn _{edge ab}	0.2 ± 0.7	2.76 ± 0.21	1.88 ± 0.01	2.8 ± 0.9
	0.2 ± 0.7	2.76 ± 0.21	1.92 ± 0.01	2.8 ± 0.9
	0.2 ± 0.7	1.84 ± 0.14	2.85 ± 0.01	2.8 ± 0.9
	0.2 ± 0.7	1.84 ± 0.14	2.91 ± 0.01	2.8 ± 0.9
	0.2 ± 0.7	2.76 ± 0.21	3.43 ± 0.01	2.8 ± 0.9
	0.2 ± 0.7	3.68 ± 0.28	3.45 ± 0.01	2.8 ± 0.9
	0.2 ± 0.7	1.44 ± 0.45	3.37 ± 0.02	2.8 ± 0.9
Mn-Mn _{corner}	-0.9 ± 0.6	2.40 ± 0.18	1.88 ± 0.01	3.0 ± 0.9
	-0.9 ± 0.6	2.40 ± 0.18	1.92 ± 0.01	3.0 ± 0.9
	-0.9 ± 0.6	1.60 ± 0.12	2.84 ± 0.01	3.0 ± 0.9
	-0.9 ± 0.6	1.60 ± 0.12	2.91 ± 0.01	3.0 ± 0.9
	-0.9 ± 0.6	2.40 ± 0.18	3.42 ± 0.01	3.0 ± 0.9
	-0.9 ± 0.6	3.20 ± 0.24	3.45 ± 0.01	3.0 ± 0.9
	-0.9 ± 0.6	1.32 ± 0.33	3.37 ± 0.02	3.0 ± 0.9
Mn-Zn	-5.5 ± 0.6	6.24 ± 0.30	1.91 ± 0.01	4.7 ± 0.7
	-5.5 ± 0.6	5.2 ± 0.25	2.87 ± 0.01	6.2 ± 0.6
	-5.5 ± 0.6	2.08 ± 0.10	3.42 ± 0.01	4.7 ± 0.7
	-5.5 ± 0.6	4.16 ± 0.20	3.49 ± 0.03	4.7 ± 0.7
	-5.5 ± 0.6	1.04 ± 0.05	3.57 ± 0.01	4.7 ± 0.7

Table S7. EXAFS fitting results of pristine and cycled $\alpha\text{-MnO}_2$ cathodes.

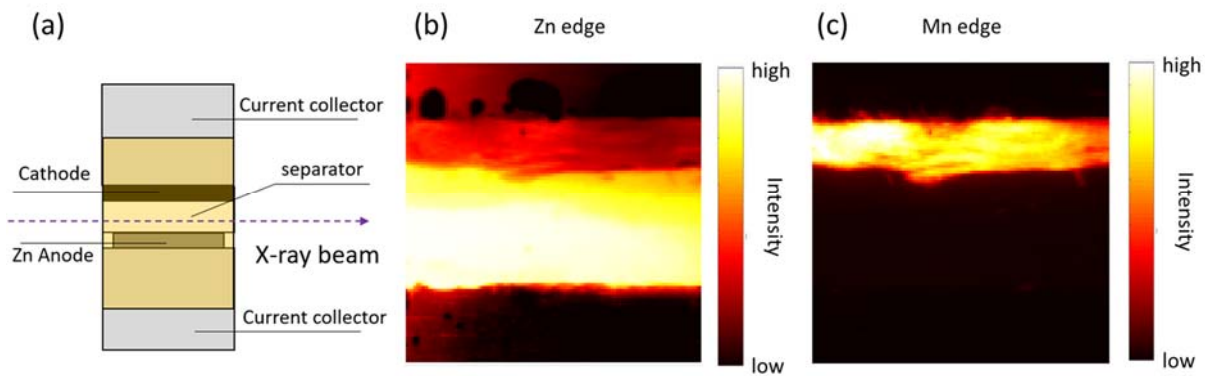


Figure S9. (a) Configuration schematic of the *operando* cell used for XRF measurements. XRF maps of the Zn/MnO₂ cell before discharge collected at the (b) Zn K-edge and (c) Mn K-edge.

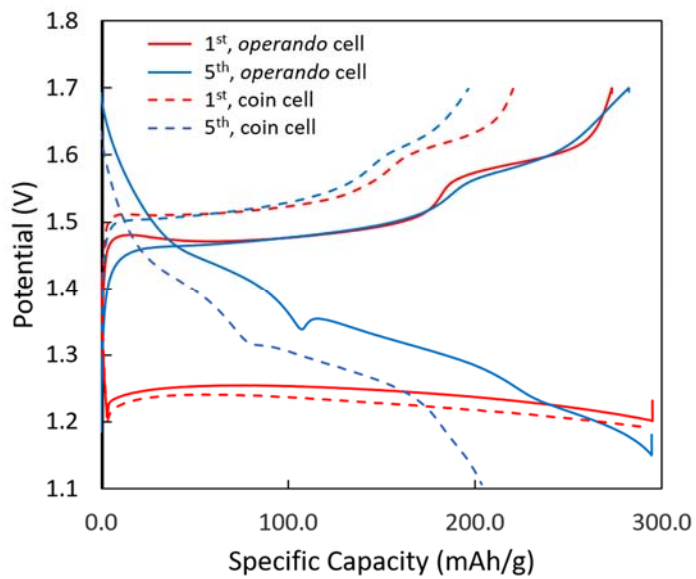


Figure S10. Electrochemistry comparison between coin cell and *operando* cell.

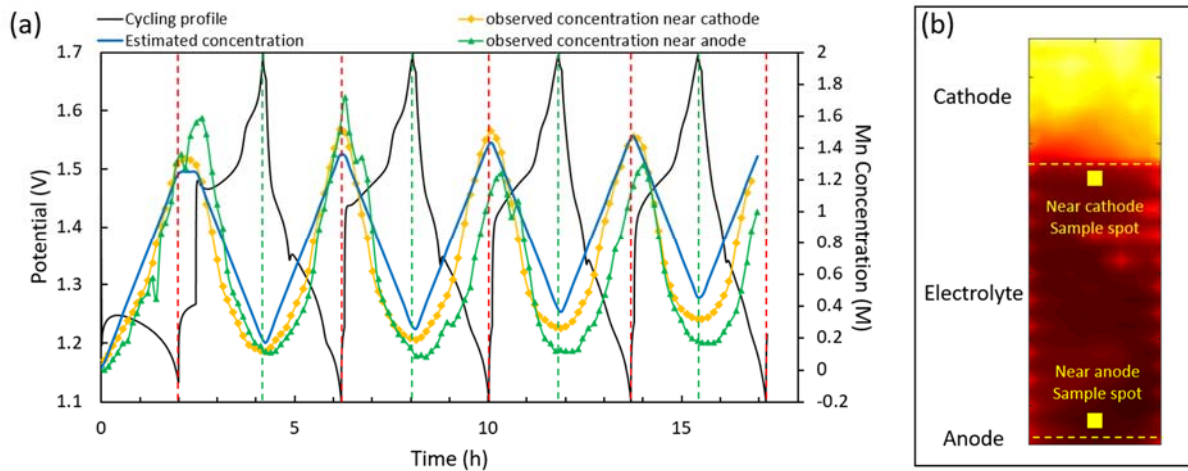


Figure S11 **(a)** Operando cell electrochemistry, observed local Mn concentration and estimated Mn concentration plotted together. **(b)** Mn-edge XRF map showing the sampling spot for local Mn concentration.

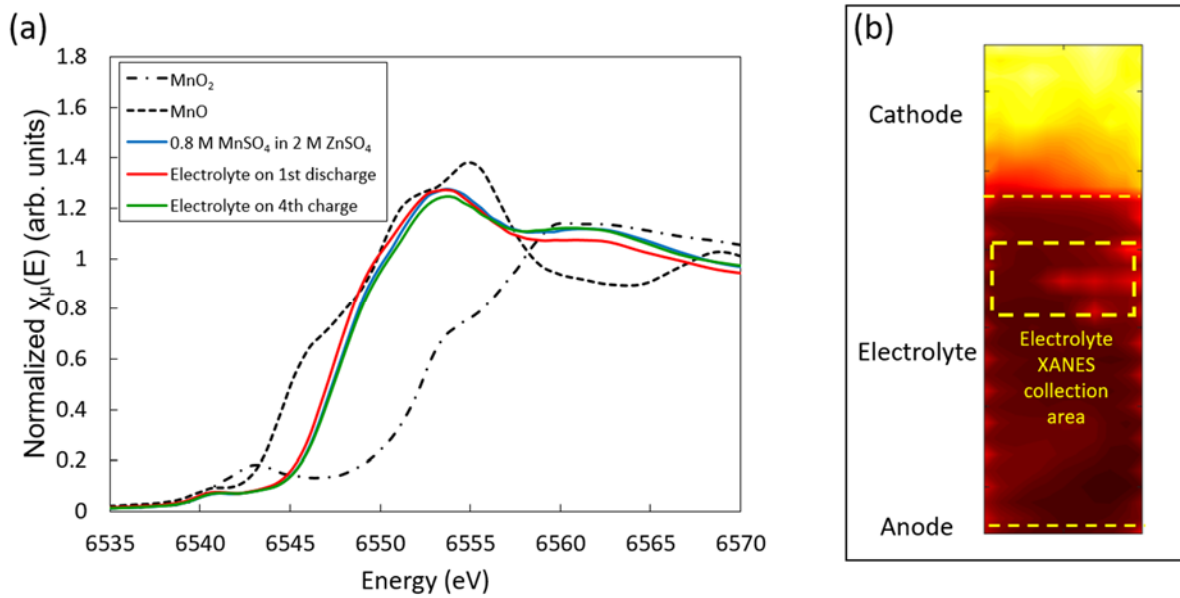


Figure S12 **(a)** Operando Mn K-edge XANES collected in the electrolyte compared with standard $\text{MnSO}_4 + \text{ZnSO}_4$ solution and other standards. **(b)** Mn K-edge XRF map demonstrating the XANES collection area in the electrolyte.

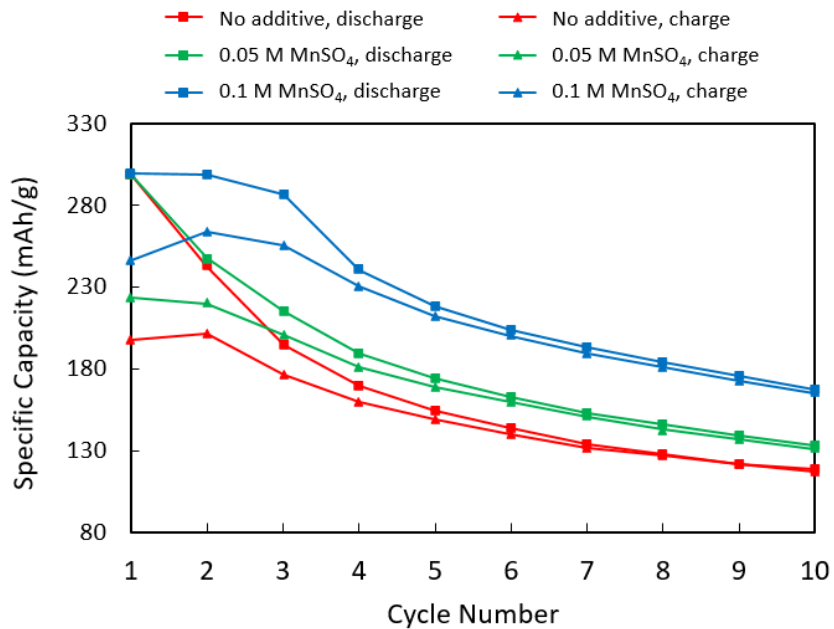


Figure S13. Specific discharge and charge capacities of Zn/MnO₂ cells with 2 M ZnSO₄, 2 M ZnSO₄ + 0.05 M MnSO₄, and 2 M ZnSO₄ + 0.1 M MnSO₄ electrolyte cycled at 150 mA/g. Initial discharge capacities of Zn/MnO₂ cells increase with an increase in MnSO₄ electrolyte additive. There is an observable concentration dependence for both charge and discharge capacities at all cycles with the addition of MnSO₄ to the electrolyte, demonstrating that MnSO₄ can provide added capacity to the cells.

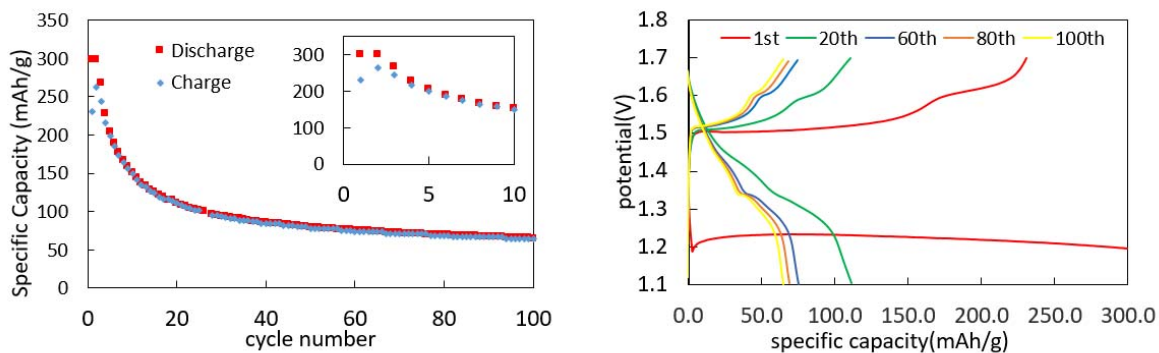


Figure S14. Extended cycling under 150 mA/g test conditions.